

Multi-Criteria Decision Analysis for Flood Risk Assessment in Informal Settlements: A Case Study from Northern Morocco

Ikram Ouakkas^{1*}, Asmae Taftafe^{2*}, Najib bahi³ and Adnane Habib⁴

¹ESGT, Le CNAM, 72000 Le Mans, France

²Department of Earth Sciences, Faculty of Sciences and Techniques, University Sultan Moulay Slimane, 23000 Béni Mellal, Morocco

³Bahi Najib Company, Temara, Morocco

⁴ESIM, Polydisciplinary Faculty of Sidi Bennour, Chouaib Doukkali University, El Jadida, Morocco

*Corresponding author

Ikram Ouakkas and Asmae Taftafe ESGT, Le CNAM, 72000 Le Mans, France and Department of Earth Sciences, Faculty of Sciences and Techniques, University Sultan Moulay Slimane, 23000 Béni Mellal, Morocco.

Received: July 23, 2025; **Accepted:** July 28, 2025; **Published:** August 08, 2025

ABSTRACT

Floods are among the most devastating natural hazards, particularly in informal urban settlements where infrastructure and planning are often inadequate. This study focuses on the Chraka area, an informal settlement located in the Tangier-Tétouan-Al Hoceïma region of northern Morocco, with the aim of assessing flood risk impact using a geospatial-based approach that integrates satellite imagery, hydrological data, and Geographic Information Systems (GIS). The methodology involves preparing flood-determining criteria within a GIS framework, applying the Analytic Hierarchy Process (AHP) used to assign weights to each factor. The resulting risk map delineates flood-prone zones, which were overlaid with building footprint data to classify structures into three risk levels: critical, moderate, and low. Although field validation was not conducted, the study provides essential insights for local authorities and stakeholders to support risk prevention and urban planning strategies. The approach demonstrates the potential of geospatial tools to serve as decision-support systems in contexts where field validation is limited. Future research could enhance predictive capabilities by integrating deep learning models for flood forecasting in similar contexts.

Keywords: Flood Risk, Informal Settlements, Remote sensing, GIS, AHP, Chraka, Watershed

Introduction

Flooding is among the most frequent and destructive natural hazards globally, particularly impacting informal urban settlements where infrastructure and planning are often inadequate. The city of Tangier has experienced several significant flood events in recent years, notably the devastating flood of February 8, 2021, which resulted in 28 fatalities, primarily women working in an illegal underground textile factory. This incident underscores the vulnerability of informal settlements like Chraka, located in the southern periphery of Tangier, to flood hazards [1].

Chraka, as an informal settlement, lacks basic infrastructure and urban regulation, making it particularly susceptible to flood hazards due to its topography, soil characteristics, and unplanned urban sprawl. Assessing flood risk in such contexts becomes both a scientific challenge and a societal necessity [2].

Traditional methods of flood risk analysis often rely on in situ surveys and hydrological instrumentation. However, recent advances in geospatial sciences offer new possibilities for remote and rapid flood modeling. Studies have demonstrated the effectiveness of integrating Geographic Information Systems (GIS), remote sensing, and machine learning techniques for flood risk assessment in various regions of Morocco. For instance, in the Dades Wadi watershed, a combination of GIS and the Analytical Hierarchy Process (AHP) was employed to assess flood risk, highlighting the potential of such integrated approaches [3].

Citation: Ikram Ouakkas, Asmae Taftafe, Najib bahi, Adnane Habib. Multi-Criteria Decision Analysis for Flood Risk Assessment in Informal Settlements: A Case Study from Northern Morocco. *J Envi Sci Agri Res.* 2025. 3(4): 1-5. DOI: doi.org/10.61440/JESAR.2025.v3.78

In Tangier, machine learning techniques like K-means clustering and fuzzy logic have been utilized to predict flood-prone areas, demonstrating the applicability of these methods in the absence of comprehensive flood inventory maps. These approaches underscore the potential of geomatics tools as decision-support systems in contexts where field validation is limited [4].

This study aims to leverage these tools, specifically satellite data, hydrological modeling, and GIS, to produce a spatial assessment of flood risk in the Chraka settlement. The analysis includes a classification of at-risk structures based on their exposure to modeled flood extents, with three degrees of severity: critical, moderate, and low.

Beyond its scientific contribution, the study serves as a decision-making product for local authorities and urban planners, while also raising awareness among the population regarding the importance of respecting urban development regulations. In future work, the integration of deep learning models could further enhance the predictive capacity of such approaches, especially in rapidly changing environments where early warning systems are lacking.

The framework of this paper outlines the methodological approach, including data sources and analytical techniques used for this assessment. It then presents the key findings of the spatial analysis conducted in the Chraka settlement, followed by a discussion on the implications for urban planning and risk management.

Materials And Methods

To assess flood risk in the Chraka watershed, a Multi-Criteria Decision Analysis (MCDA) approach was used to evaluate and compare different alternatives or options based on a set of predefined criteria (Denis 1990). The MCDA was employed using the AHP [5]. Nine environmental and hydrological parameters were selected based on their relevance in flood risk assessment: Topographic Wetness Index (TWI), elevation, slope, distance from river, drainage density, precipitation, NDVI, land use, and soil type (Figure 1).

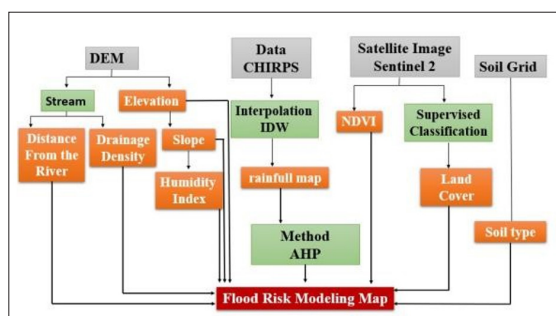


Figure 1: Workflow Methodology

Each criterion was assigned a relative weight based on expert knowledge and literature, following pairwise comparisons within the AHP framework (Figure 2). The weights assigned to each criterion were derived from the normalized principal eigenvector of the pairwise comparison matrix using AHP:

- Distance from river (14.5%) and TWI (14.0%) emerged as the most influential factors due to their strong correlation with surface runoff and water accumulation,

- Precipitation (14.0%) and elevation (12.5%) also played major roles in defining flood-prone areas.
- Slope (10.0%), drainage density (10.0%), NDVI (8.5%), land use (8.5%), and soil type (8.0%) had a comparatively lower impact but remained important contributors to the overall flood risk assessment.

The individual raster layers were normalized and reclassified before being combined using a weighted linear combination (WLC) in a GIS environment. The resulting flood hazard map was then intersected with building footprint data to assess flood risk at the building footprint level.

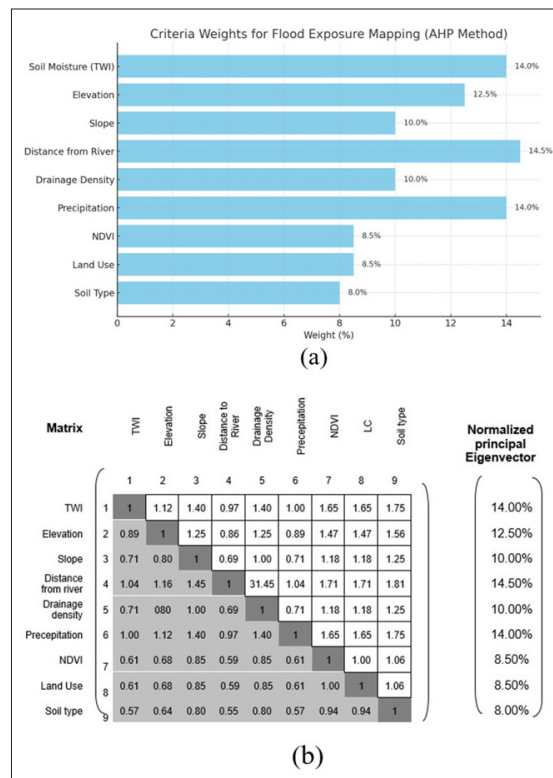


Figure 2: (a). Criterion's influence on the flood hazard. (b) The pairwise comparison matrix of the nine criteria for the AHP process.

Study Area

The study area is located within one of the sub-watersheds of the Tangier basin, characterized by the main watercourses of Oued Mharhar, Oued Hachef, and Oued Ayacha, which form narrow valleys at their outlets along with several tributaries (Figure 3). These basins are marked by steep slopes in the upstream sections and wide floodplains downstream, where runoff accumulates during heavy rainfall events [6]. The predominant geological formations consist of impermeable or low-permeability clay-schist. The only significant aquifer is the Charf El Akab, which benefits from artificial recharge through treated waters from neighboring wadis [7].

This particular basin covers an area of 1,433 hectares, with a maximum width and length of 4 kilometers in the north-south and east-west directions, respectively.

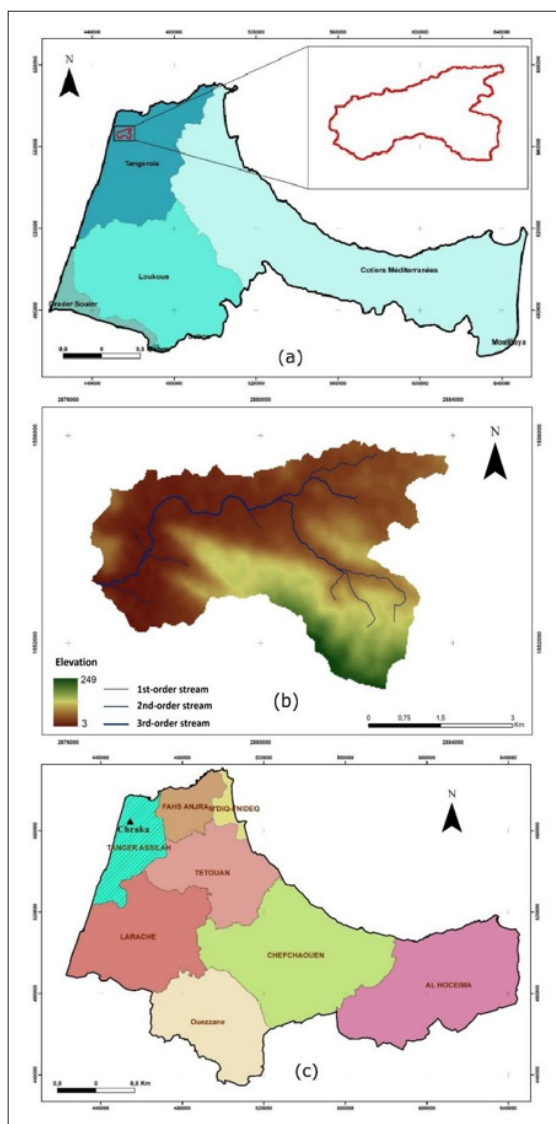


Figure 3: (a) Location of the basin (b) Elevation and stream network classified by order (c) Location of the Study Area.

Within this basin lies the village of Chraka ($35^{\circ} 41' 6''\text{N}$, $5^{\circ} 54' 10''\text{W}$), situated southwest of Tangier (**Erreur ! Source du renvoi introuvable.**), near the hamlet of Al Farihiyine and the village of Gueznaia, covering an area of 405.8 hectares. The village occupies a rugged coastal terrain with steep slopes and significant elevation differences. Economically, the area suffers from a lack of major activity, which has led to the emergence of a slum composed of unauthorized permanent constructions on illegally subdivided land. Contributing factors include unemployment, poverty, internal migration, and social inequality, which make this zone particularly vulnerable to flood-related hazards (RFI 2016).

Data Used

We primarily used the Sentinel-2 Level-1C (MSIL1C) dataset that consists of multispectral optical imagery acquired by the Sentinel-2 satellite, which is part of the European Space Agency's Copernicus program. The Level-1C product provides Top-Of-Atmosphere (TOA) reflectance data that are already orthorectified and projected in UTM coordinates. The imagery includes 12 spectral bands, covering the visible to the short-wave infrared (SWIR) [8]. From this dataset, we derived the

NDVI (Figure 4.b), which was used to assess vegetation health and coverage. NDVI is a key criterion in flood modeling, as dense vegetation can reduce runoff and act as a buffer. We also extracted a simplified land cover classification (Figure 4.d), distinguishing between buildings, vegetation, and bare soil, to characterize surface properties and their influence on infiltration and runoff.

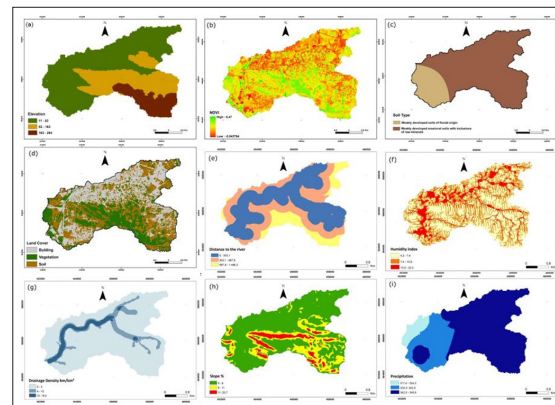


Figure 4: Derived maps used for the AHP analysis. (a) Elevation. (b) NDVI. (c) Soil type. (d) Land cover. (e) Distance to the river. (f) Humidity index. (g) Drainage density. (h) Slope. (i) Precipitation.

To estimate precipitation, we used CHIRPS (Climate Hazards Group InfraRed Precipitation with Station data), which provides high-resolution gridded rainfall data. The dataset used in this study has a spatial resolution of ~ 5 km. From it, we produced precipitation map (Figure 4.i), which shows relatively high precipitation values (342.5 – 345.9 mm) dominating the basin area, a significant factor in the analysis of flood potential [9].

We also used a SRTM (Shuttle Radar Topography Mission) Digital Elevation Model (DEM) (Figure 4.a), with a spatial resolution of 30 meters. This DEM was used to generate several key topographic and hydrological variables, including:

- Distance to the river (Figure 4.e): calculated as the Euclidean distance from each pixel to the nearest stream, indicating the exposure of structures to potential overflow.
- Humidity Index (Figure 4.f): derived from slope and wetness parameters, indicating zones with higher potential for water accumulation.
- Drainage Density (Figure 4.g): expressing the total length of streams per unit area (km/km^2), used to evaluate the landscape's drainage capacity.
- Slope (%) (Figure 4.h): showing areas with steep inclines where runoff is accelerated, increasing flood risk in downslope zones.

Soil type (Figure 4.c) was extracted from the Soil Grids global dataset (ISRIC). The study area is mainly composed of weakly developed soils of fluvial origin and weakly developed erosional soils with inclusions of raw minerals, which typically have low permeability and contribute to increased surface runoff.

Additionally, a map of the informal settlement area known as Chraka (Figure 5) was integrated into the study. This dataset was obtained as part of a photogrammetric mission using drone

imagery with a 30 cm spatial resolution. The high resolution allowed for the accurate extraction of building contours, essential for evaluating flood risk at the building level.

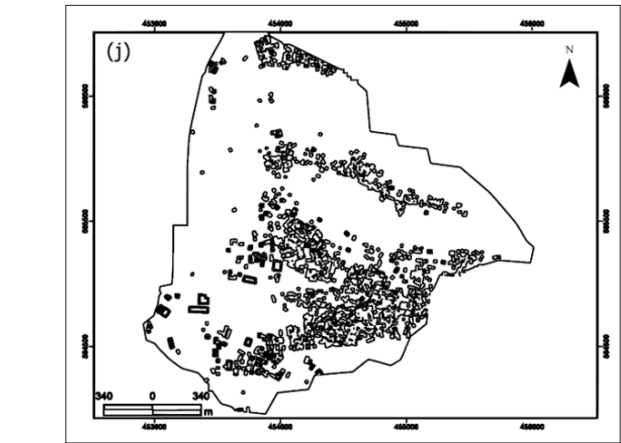


Figure 5: Chraka’s building footprint map

All these datasets, summarized in

Table 1, were integrated in a GIS environment and resampled to a common spatial resolution of 10 m, except for the building shapefile, which was used at its original resolution for detailed local analysis.

Table 1: Summary of the datasets used

Source datasets	Resolution	Derived products used	Reference
Sentinel-2 (ESA)	10 m	NDVI, Land cover	Copernicus Open Access Hub
SRTM (USGS)	30 m	Slope, Drainage density, Distance to the river	USGS Earth Explorer
CHIRPS (Climate Hazards Group)	~5 km	Mean Annual Rainfall	CHIRPS Data
SoilGrids	30 m	Soil type	SoilGrids

Results and Discussions

The integration of detailed hydrological and environmental variables allowed for a spatially explicit mapping of flood risk across the watershed (Figure 6.a). The results reveal a clear concentration of high-risk zones along riverbanks and in topographically low-lying areas, where water accumulation is more likely to occur. These areas, represented in red, exhibit increased vulnerability due to their proximity to drainage paths and the limited presence of protective vegetation. Medium risk zones dominate the central portion of the watershed, while low-risk areas are mainly located in the southern parts, characterized by higher elevations and denser vegetation cover.

The use of high-resolution building footprint data, obtained through photogrammetry, significantly improved the accuracy of

building-level risk-mapping analysis (Figure 6.b) by providing further insights into the exposure of individual buildings to flood hazards. The detailed footprint map shows a substantial number of buildings situated within medium and high-risk zones, reflecting the critical vulnerability of this informal settlement. The spatial overlap between building locations and risk levels reveals that the western and northwestern parts of the village are the most exposed, emphasizing the urgent need for risk mitigation and land- use planning interventions in these sectors. However, the study faced several limitations related to data availability and quality. One of the main constraints was the lack of validation data, such as historical flood extent maps, high-frequency hydrological records, or field-verified flood impact reports. This limited our ability to quantitatively validate the model's accuracy and assess its predictive performance.

Moreover, while precipitation was one of the most influential variables, the spatial resolution and temporal coverage of the precipitation dataset used in this study were not optimal. A finer resolution data, preferably derived from local weather stations or radar-based systems, could have significantly improved the delineation of high-risk zones.

Despite these limitations, the results offer valuable insights into the spatial dynamics of flood risk, especially in informal settlement areas. The AHP approach proved effective in integrating diverse datasets, but future work should consider incorporating uncertainty analysis and real-world validation to enhance the robustness of the findings.

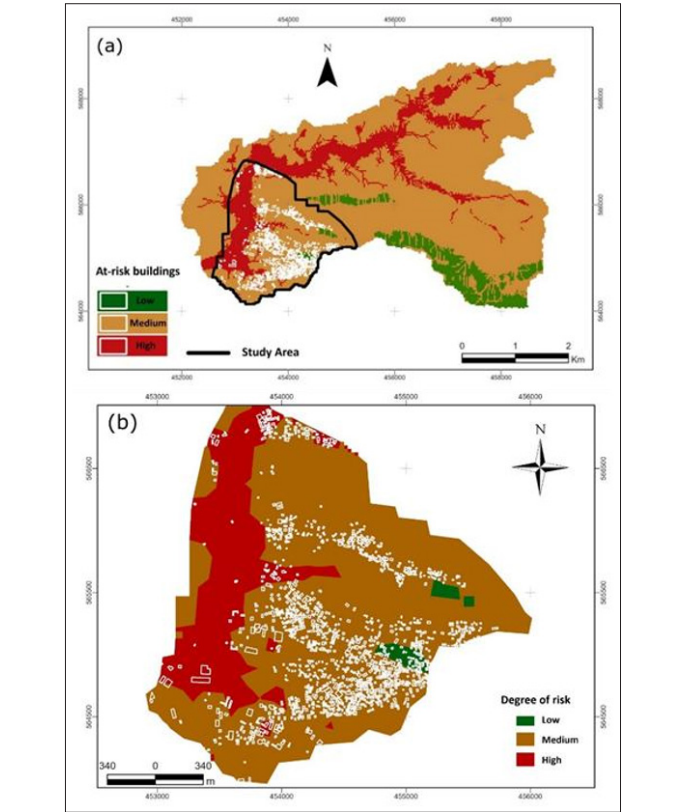


Figure 6: Building flood risk maps in the Chraka area. (a) At-risk building distribution within the entire watershed. (b) Detailed zoom on the study area showing building footprints and flood risk zones

Conclusions

The integration of high-resolution photogrammetric data and flood modeling outputs enabled the production of a detailed flood risk map for the Chraka informal settlement. The results revealed that a significant number of buildings, within informal areas, fall within zones classified as medium to high flood risk.

This study highlights the value of combining geospatial analysis and the AHP method to support urban planning and disaster preparedness in data-scarce environments. Despite the absence of validation data and the limitations of course-resolution precipitation datasets, the model successfully identified priority zones for intervention.

To further enhance accuracy, future research should incorporate higher-resolution meteorological data, field-based validation, and socio-economic vulnerability indicators. Integrating deep learning models could also improve predictive capabilities in rapidly urbanizing and climate-sensitive regions.

This approach contributes not only to the scientific understanding of flood risk dynamics in informal settlements but also serves as a decision-support tool for local authorities, urban planners, and disaster risk managers.

References

1. El Jazouli A, Barakat A, Khellouk R, El Morhit M. Multivariate analysis and machine learning approach for mapping the variability and vulnerability of urban flooding: the case of Tangier City, Morocco. *Water*. 2021. 13: 182.
2. Snoussi M, Ouchani T, Khouakhi A, Niang-Diop I. Impacts of sea-level rise on the Moroccan coastal zone: quantifying coastal erosion and flooding in the Tangier Bay. *Geomorphology*. 2009. 107: 32-40.
3. Aichi A, Barakat A, El Jazouli A. Integrated GIS and analytic hierarchy process for flood risk assessment in the Dades Wadi watershed (Central High Atlas, Morocco). *Results in Earth Sciences*. 2024. 100019.
4. Wassima M, Bencheckroun H, El Fahim H, Bouziane L. Enhancing flood risk assessment in northern Morocco with tuned machine learning and advanced geospatial techniques. *Journal of Geographical Sciences*. 2024. 34: 2477-2508.
5. Saaty TL. The analytic hierarchy process: planning, priority setting, resource allocation. s.l.: s.n. 1980.
6. Alessio S, El Morhit M, Idrissi L. Gender-sensitive climate risk assessment of the Tangier- Tétouan-Al Hoceima Region, Morocco. s.l.: s.n. Denis B., 1990. Building criteria: a prerequisite for MCDA. *Readings in Multiple Criteria Decision. Aid*. 2022. 1-9.
7. Felicita S, Dini F, Rachid A. A socio-economic and environmental analysis of changes and sustainable management of Mediterranean coastal water bodies. s.l.: s.n. RFI, 2016. Maroc: Tanger, une ville-bidonville. 2021. <https://www.rfi.fr/fr/emission/20160222-maroc-tanger-une-ville-bidonville>.
8. European Space Agency. Copernicus Sentinel-2 Collection 1 MSI Level-1C (L1C). 2021. <https://sentinels.copernicus.eu/sentinel-data-access/sentinel-products/sentinel-2-data-products/collection-1-level-1c>.
9. Satellite Imaging Corporation. Sentinel-2A Satellite Sensor (10m). 2022. <https://www.satimagingcorp.com/satellite-sensors/other-satellite-sensors/sentinel-2a>.